1976ApJ...209...22T

THE ASTROPHYSICAL JOURNAL, 209:22–34, 1976 October 1
© 1976. The American Astronomical Society. All rights reserved. Printed in U.S.A.

THE ANGULAR MOMENTUM PROPERTIES OF GALAXIES IN RICH CLUSTERS

LAIRD A. THOMPSON
Kitt Peak National Observatory*
Received 1976 February 11

ABSTRACT

In order to study the rotational angular momentum characteristics of galaxies in rich clusters, ellipticities and major-axis position angles have been measured for the largest 100 to 150 galaxies in eight rich clusters: Virgo, A119, A400, A1656 (Coma), A2147, A2151 (Hercules), A2197, and A2199. The following results are reported: (1) galaxies in the cluster A2197 appear to be systematically aligned, (2) elliptical galaxies in Coma seem to be aligned radially with respect to the cluster core, (3) cluster galaxies and local "field" galaxies have similar ellipticity distributions, and (4) S0 galaxies may be a mixture of objects with intrinsic ellipticities of 3.5 and 7. It is shown that a galaxy's internal angular momentum remains undisturbed from primordial times unless the galaxy is confined to the core of a rich cluster. These new results seem to be consistent with models of galaxy formation which involve the collapse and subsequent fragmentation of massive cluster-size clouds of gas.

Subject headings: galaxies: clusters of — galaxies: formation — galaxies: structure

I. INTRODUCTION

No one knows for sure why or how galaxies started to rotate. The theoretical explanations are numerous, and generally they can be placed in one of two categories. The first category contains the primordial turbulence theories (e.g., von Weizsäcker 1951; Ozernoi and Chernin 1968, 1969; Doroshkevich 1973*a*; Jones 1973), and the second category contains the gravitational tidal interaction theories (e.g., Hoyle 1949; Peebles 1969, 1971*a*; Silk and Lea 1973). In the present investigation the problem of galaxy rotation is approached empirically with emphasis placed on two specific questions: (1) Are the rotational properties of galaxies identical in all regions of space (i.e., *homogeneity*)? (2) Are galaxies' angular momentum vectors distributed *isotropically* in the sense that every galaxy is unaware of how its nearest neighbors are rotating? The answers to these two questions should help in deciding which of the theoretical explanations is most reasonable.

The first question (homogeneity) can be answered by obtaining and comparing the intrinsic ellipticity distributions for specific samples of galaxies located in various regions of space. If galaxies in one region have an intrinsic ellipticity distribution different from that of galaxies in another region, then it might be concluded that the angular momentum transfer process was not universally homogeneous. This test will be used to compare the local sample of "field" galaxies with rich cluster galaxies and to compare galaxies in one cluster with those in another. The results of the comparisons must be interpreted very cautiously because the ellipticity of a galaxy depends not only on its initial protogalaxy angular momentum, but also on the detailed way in which the protogalaxy collapsed to form stars. Hopefully, all difficulties can be circumvented by assuming that the galaxies of any one morphological type follow similar evolutionary histories. Using this assumption, ellipticals in the field will be compared with ellipticals in clusters—S0's in the field with S0's in clusters, etc.

The isotropy question will be tested by looking for systematic alignment effects among galaxies in rich clusters using the position angle of each galaxy's major axis to indicate its orientation.[1] There is a reasonable physical justification for making the orientation survey on cluster-size aggregates. In the expanding big-bang cosmologies the adiabatic perturbation model predicts that the first mass scales to become unstable to Jeans collapse will be those that are comparable to galaxy cluster masses (cf. Field 1965; Icke 1973). If the origin of galaxy rotation is related in any way to this initial cluster collapse phase, systematic galaxy alignment might be expected (cf. Sunyaev and Zel'dovich 1972; Doroshkevich 1973*a*; Icke 1973). Although the following analysis will include a review of previous studies dealing with the alignment of galaxies in clusters, nothing will be said of the numerous and ambiguous field galaxy alignment studies. A complete discussion and review of the field galaxy alignment data is given by Hawley and Peebles (1975).

The galaxy rotation study presented below is based on new measurements of galaxy ellipticity, major-axis

* Operated by the Association of Universities for Research in Astronomy, Inc., under contract with the National Science Foundation.

[1] A full three-dimensional orientation analysis would be ideal, but unfortunately it is beyond the scope of the data that are now available. Each galaxy's inclination to the plane of the sky can be determined using its apparent and intrinsic ellipticities, but uncertainty in specifying the intrinsic ellipticity adds undue complication. The present study will involve only major-axis position-angle orientations.

© American Astronomical Society • Provided by the NASA Astrophysics Data System

1976ApJ...209...22T

TABLE 1

Basic Cluster Parameters

Cluster	Mean Cluster Redshift	Cluster Radius	Galaxy Diameter Limit	Plate Seeing	Total Galaxy Sample	R & S Cluster Type	B & M Cluster Type
Virgo	0.0381	6°.619	137".0	3".0	65	-	III
A119	0.0417	0.651	13.5	2.5	96	C	II-III
A400	0.0231	1.133	23.3	2.0	79	I	II-III
A1656	0.0230	1.138	23.6	3.0	152	B	II
A2147	0.0377	0.714	15.0	3.5	128	F	-
A2151	0.0360	0.745	15.4	3.5	142	F	II
A2197	0.0303	0.876	18.1	2.0	152	L	II
A2199	0.0312	0.852	17.7	2.0	161	cD	I

position angle, and morphology for the largest 100–150 galaxies in eight rich clusters. To supplement these new results, the analysis also includes a discussion of the local "field" galaxy ellipticity distributions found by Sandage, Freeman, and Stokes (1970). In the following section (§ II) the sample of eight clusters is briefly discussed and the galaxy measuring procedures are described. Section III contains the galaxy orientation analysis along with a discussion of other cluster alignment studies. In § IV, the galaxy ellipticity distributions are presented and analyzed. Finally, § V contains a general discussion of how these observations are related to the origin of galaxy angular momentum and the formation of galaxies.

II. CLUSTER SELECTION, GALAXY SELECTION, AND MEASURING PROCEDURES

The eight clusters included in this survey are listed in Table 1. They were selected using the following criteria: (1) all clusters had to have an Abell richness $R \geqslant 1$; (2) they had to fall outside the galactic plane with $|b^{II}| \geq 40°$; (3) the mean cluster redshift had to be fairly small, $z \leq 0.05$; and (4) except for the Virgo cluster, each cluster had to fall within the field of a single Palomar Sky Survey plate. In addition to these restrictions, an effort was made to include a wide variety of cluster types using the classification schemes of Bautz and Morgan (1970) and Rood and Sastry (1971).

All galaxy measurements were made on the Kitt Peak National Observatory (KPNO) glass plate copies of the Palomar Sky Survey. Position angle and ellipticity measurements were taken from the red 103a-E plates. The galaxy morphology was determined using both the red and blue Sky Survey plates, and, whenever possible, it was supplemented by better plate material or by previously published determinations (Burbidge and Burbidge 1959; Rood and Baum 1967).

After selecting the eight clusters and choosing appropriate cluster centers, a circular survey area was defined using a cluster radius

$$R = 90'' \frac{(1+z)^2}{z}, \qquad (1)$$

where z is the mean cluster redshift (listed in Table 1). This angular radius R is scaled so that it corresponds to a metric length of approximately $R = 1.5$ Mpc at the distance of each cluster. Within this survey region all galaxy-like images on the Sky Survey plates were identified, and in a rough preliminary survey of major-axis diameters it was decided that the final galaxy sample should include every galaxy with a corrected major-axis diameter greater than or equal to

$$D = 0''.5 \frac{(1+z)^2}{z} = \frac{7.5 \text{ kpc}}{h}, \qquad (2)$$

where $h \equiv$ Hubble's constant/(100 km s^{-1} Mpc^{-1}).

Galaxy major and minor diameters were measured using a reticle scale by projecting an enlarged image of the Sky Survey plate on a ground glass screen. These visual diameters were corrected for systematic measuring effects following the procedures described by Holmberg (1946). The two diameters (and hence the ellipticities) can be considered as approximate isophotal measurements. The apparent major-axis diameters were corrected to face-on values following the method described by Holmberg (1946) and later by Heidmann, Heidmann, and de Vaucouleurs (1972). If a and b are the measured major and minor axes diameters, respectively, and D and $D(O)$ the apparent and face-on galaxy diameters, respectively, then

$$D(O) = D(a/b)^{-n},$$

where $n = 0.15$. This latter value of n was derived empirically using the data described herein; it agrees well with previous determinations (cf. Heidmann, Heidmann, and de Vaucouleurs 1972). Other minor corrections were made to eliminate the effects of seeing and plate-to-plate variations of galaxy diameters (only necessary in the Virgo cluster).

The accuracy of the diameter measurements depends strongly on the galaxy's apparent image density gradient. For those galaxies which blend slowly into the sky background, the diameters might have errors of approximately 10 percent. For more sharply bounded galaxies, the errors are substantially reduced. Although the diameter measurements are subject to moderate errors, note that galaxy ellipticity depends on the ratio of the major to the minor axis

$$\epsilon = 10(1 - b/a).$$

© American Astronomical Society • Provided by the NASA Astrophysics Data System

1976ApJ...209...22T

The ratio b/a is less sensitive to the galaxy image structure, and the ellipticity is therefore more accurate. For galaxies of moderate ellipticity, $\Delta\epsilon \approx \pm 0.2(1\ \sigma)$. For the extremely flat galaxies the ellipticity depends critically on the small minor-axis measurement, so that the error increases to $\Delta\epsilon \approx \pm 0.4\ (1\ \sigma)$.

The major-axis position angles were determined by aligning a rotating reticle scale, which was overlayed on the projected galaxy image, with the apparent galaxy major axis. The position angle of the rotating scale was easily determined to within $\pm 0.^{\circ}5$, so all position-angle inaccuracy can be ascribed to the difficulty of visually defining a major-axis orientation. By comparing independent sets of measurements these inaccuracies were determined to be $\pm 2^{\circ}$ $(1\ \sigma)$ for galaxies with ellipticities ≥ 5, and for the more circular galaxies with ellipticities ~ 2, the error increases to $\pm 6^{\circ}$ $(1\ \sigma)$. For the analysis described in the following sections the position-angle distributions include only those galaxies with ellipticities ≥ 2. All position angles were measured in the conventional sense, from the north through the east, with the north-south reference line taken to be the meridian passing through the cluster center.

Position-angle studies must be made carefully in order to avoid systematic measuring errors. This has been stressed by Öpik (1968) in reference to position-angle studies by Brown (1964, 1968), and the nature of these systematic measuring effects was carefully analyzed by Hawley and Peebles (1975). The present study follows closely the precepts outlined by Öpik. For each cluster area, two independent surveys were made. In each survey, major axes, minor axes, and position angles were measured for all galaxies including those with apparent diameters well below the limit defined by equation (2). In the first survey the plate was oriented with the north-south axis projected in the vertical direction. After waiting at least one week, the second survey was made with the plate rotated through 112°. This angle was chosen in an attempt to cancel any systematic measuring effects that occur at multiples of 45°. After the two surveys were completed, average values were determined for all three measured quantities. The diameters were corrected for Holmberg effects, seeing effects, and converted to face-on values. The lower diameter limit given in equation (2) was applied to the data *after* all averages and corrections were completed.

A more detailed discussion of the measuring procedures, the precise form of the Holmberg corrections, and a more complete error analysis can be found in Thompson (1974). This reference also contains a catalog which lists the final measurements adopted for each of the galaxies in this survey.

III. POSITION ANGLE DISTRIBUTIONS

The position-angle data will be used for two tests. The first will be the straightforward check for linear or parallel alignment of galaxies within each cluster sample. The second will be to test for radial alignment with respect to the direction of the cluster core. Anticipating the discussion in § V, note that in the absence of close, disruptive collisions the parallel alignment test should reflect the overall primordial orientation of the galaxies' angular momentum vectors, and that radial alignment might reflect either a primordial effect or a more recent tidal disruption of those galaxies which continually pass through the cluster core on radial orbits.

First consider the parallel alignment effect. The sample will be limited to those galaxies with ellipticities ≥ 2.0 to ensure that the position angles of all galaxies are well defined and accurate to *at least* $\pm 6^{\circ}$. For each of the eight cluster samples the position angle data are presented in Figure 1 and Table 2. Also included in Table 2 are the results of two statistical tests which check for nonrandomness. The first is the simple χ^2 test in which the observed distribution is tested against the uniform-orientation, flat distribution. Although the value of χ^2 indicates the degree of nonrandomness, it does not test for any systematic alignment trends. Hawley and Peebles (1975) introduced a convenient procedure which can be used to check for systematic effects. In this test the observed distributions are fitted with the model

$$N(\theta_i) = N_0(1 + \Delta_1 \cos 2\theta_i + \Delta_2 \sin 2\theta_i)\,,$$

where $N(\theta_i)$ is the number of galaxies observed to fall at the position angle θ_i, where $N_0 = \sum_i N(\theta_i)$, and Δ_1 and Δ_2 are coefficients that describe the deviation from nonrandomness. For position angle distributions divided into 12 bins

$$\Delta_1 = \frac{\sum N(\theta_i) \cos 2\theta_i}{6N_0}\,,$$

$$\Delta_2 = \frac{\sum N(\theta_i) \sin 2\theta_i}{6N_0}\,.$$

The probability that the total amplitude of the distribution $\Delta = (\Delta_1^2 + \Delta_2^2)^{1/2}$ exceeds the observed value Δ is then $P(>\Delta) = \exp(-3N_0\Delta^2)$. Table 1 lists the coefficients Δ_1 and Δ_2 as well as the probability P.

It is quite obvious from the plot in Figure 1 and the statistical analysis summarized in Table 2 that the galaxies in the cluster A2197 appear to be preferentially aligned. The probability for the random occurrence of this distribution is well below 10^{-3}. In an effort to confirm this result, the measurements were repeated using the blue (103a-O) Sky Survey plate of the cluster. The new analysis was made more than 6 months after the initial measurements so no "memory bias" should be present, and the same measuring procedures were followed as described above. Note that this sample of galaxies is totally independent of the other. Galaxies near the diameter limit defined in equation (2) can slip into or out of the sample, depending on how their total diameter depends on color. The blue galaxy data are listed in Table 2 and plotted in Figure 2. The alignment effect is still present with a peak in the distribution at 90°–100°, but statistically it is less convincing. Using the amplitude test, the distribution appears to be nonrandom at the 7 percent level, remarkably less random than any of

© American Astronomical Society • Provided by the NASA Astrophysics Data System

1976ApJ...209...22T

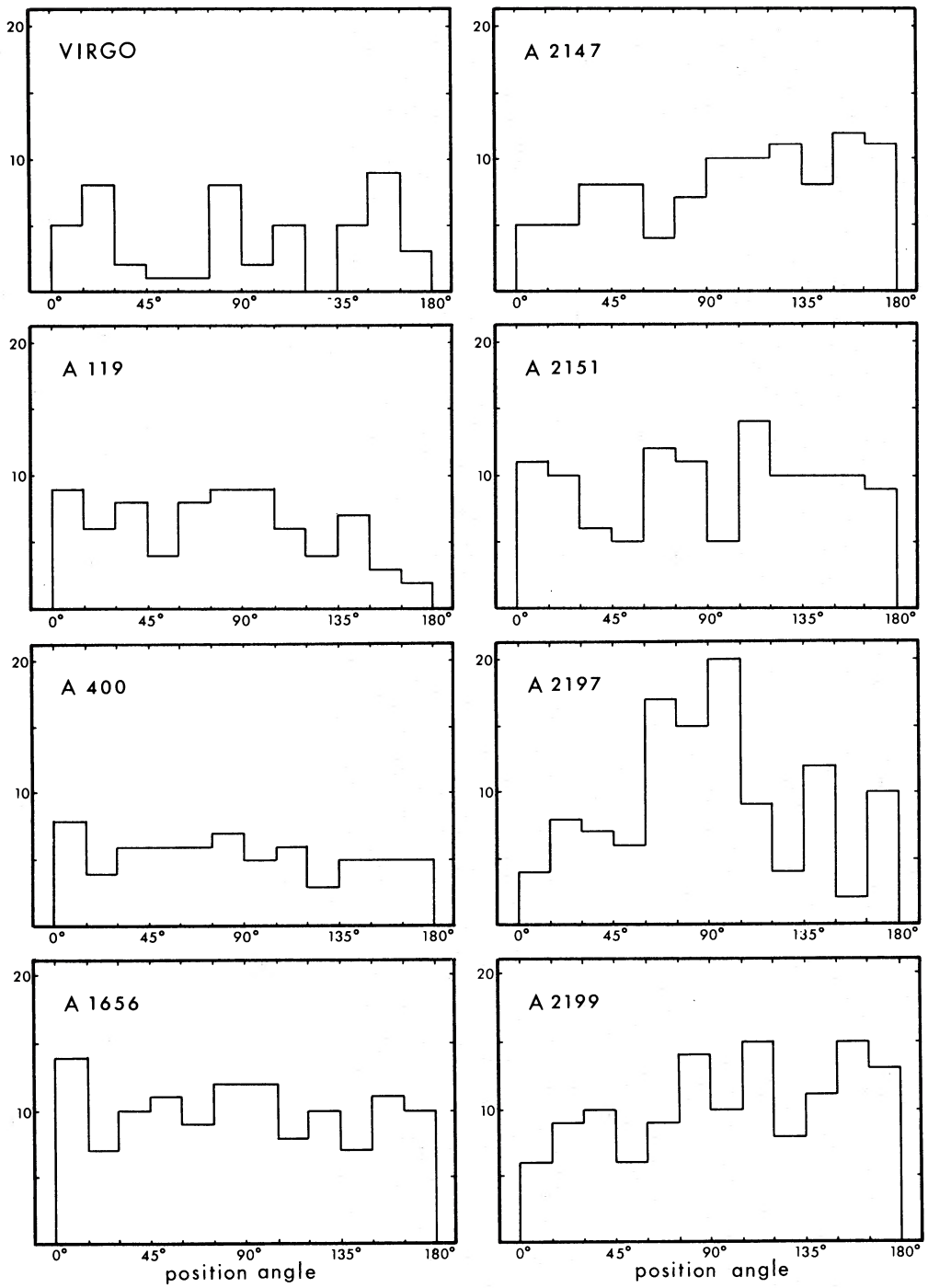

FIG. 1.—Histogram plot showing the number distribution of galaxy major-axis position angles for the eight clusters studied. A north-south orientation corresponds to a position angle of 0°; east-west, to 90°.

© American Astronomical Society • Provided by the NASA Astrophysics Data System

TABLE 2

Position Angle Distributions

Cluster	0°	15°	30°	45°	60°	75°	90°	105°	120°	135°	150°	165°	Σ	Ave.	χ^2	χ^2 Prob.	Δ_1	Δ_2	Δ Prob.
Virgo	5	8	2	1	1	8	2	5	0	5	9	3	49	4.08	25.204	0.9%	0.302	-0.139	26%
A119	9	6	8	4	8	9	9	6	4	7	3	2	75	6.25	10.920	45.0	-0.226	0.168	23
A400	8	4	6	6	6	7	5	6	3	5	5	5	66	5.50	3.455	98.3	-0.019	0.135	74
A1656	14	7	10	11	9	12	12	8	10	7	11	10	121	10.08	4.851	93.8	-0.005	0.046	93
A2147	5	5	8	8	4	7	10	10	11	8	12	11	99	8.25	9.242	58.1	-0.008	-0.291	12
A2151	11	10	7	6	12	11	5	14	10	10	10	9	115	9.58	7.400	76.6	-0.002	-0.106	72
A2197	4	8	7	6	17	15	20	9	4	12	2	10	114	9.50	35.895	0.018	-0.514	0.073	0.05
A2199	6	9	10	6	9	14	10	15	8	11	15	13	126	10.50	10.571	48.0	-0.048	-0.193	29
Total Sample -A2197	58	49	51	42	49	68	53	64	46	53	65	53	651	54.25	1.177	99.9	-0.015	-0.069	44
Virgo Suppl.	6	14	8	3	3	11	5	9	4	10	12	5	90	7.50	20.133	4.4	0.176	-0.087	42
A2197 Blue	9	10	6	11	9	15	14	11	8	7	4	9	113	9.42	11.354	41.4	-0.291	0.089	7.3

© American Astronomical Society • Provided by the NASA Astrophysics Data System

1976ApJ...209...22T

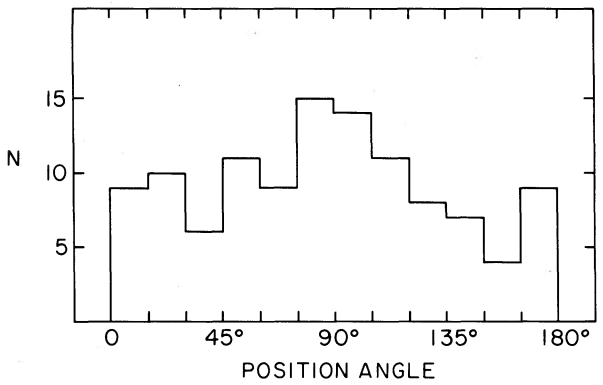

FIG. 2.—Remeasurement of the A2197 position angle distribution using the blue plate copy of the Sky Survey.

the other clusters. Better plate material for the cluster is now available, and a more detailed study of this region will be available soon.

The position angle distributions for the other seven clusters are apparently very flat and uniform. The Virgo cluster data indicate an anisotropy with the χ^2 test, but the sample is small since Virgo is the poorest cluster in the sample. In order to test the Virgo result more critically, the galaxy sample was increased (by lowering the diameter limit) to include a total of 90 galaxies. For the larger sample the χ^2 probability is still below 5 percent, but the Δ probability indicates complete randomness. The galaxies appear to fall into three marginally significant peaks with enhancements at position angles of 15°, 75°, and 150°.

In previously published studies of cluster galaxy alignment, there has been only one other claim of a systematic alignment effect. Rood and Sastry (1972) measured galaxy orientation in the cluster A2199 and found in their analysis a two-peaked distribution significantly nonrandom at the 2.5 percent χ^2 level. To check this result, the data in the present study were used to define a sample as identical as possible to the Rood and Sastry sample. The cluster radii were matched and the data were divided into similar position angle bins. The results are shown in Figure 3, and the systematic effects are not confirmed. The immediate suspicion is that there are measuring errors in one of the two studies, but a detailed comparison of the 103 galaxies which overlap both samples indicates that 65 have position angle differences less than 10° and 85 have differences less than 20°. The disagreement in Figure 3 appears to be due only to a different method of defining the galaxy sample. Better plate material has also been obtained for the A2199 area, and this region will soon be studied in more detail.

Brief mention should also be made of the orientation study of Kristian (1967). Using plates of six distant clusters, major-axis position angles were measured for an average of 60 galaxies in the clusters A151, A1377, A1589, A1930, A2048, and A2065. No details of the measuring procedures are given, but none of these clusters show any systematic alignment trends.

Consider next the radial position angle distributions.

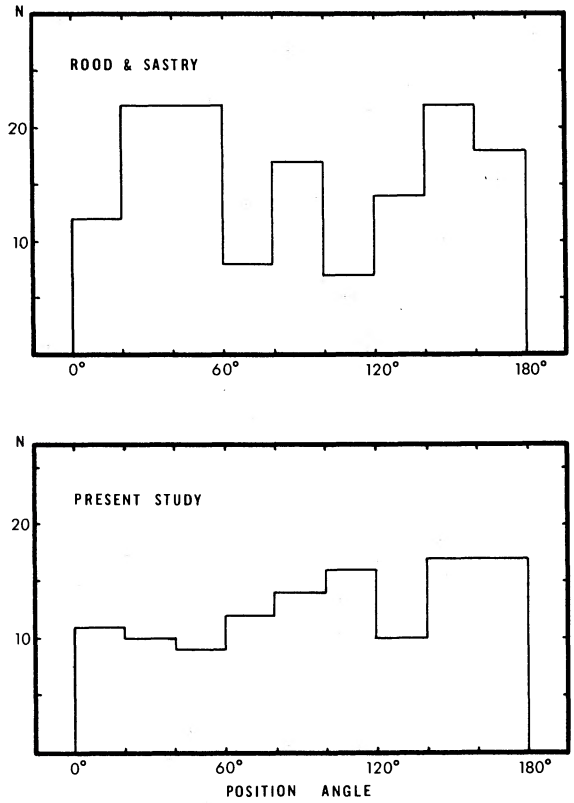

FIG. 3.—Comparison between two studies of galaxy major-axis position angles for the cluster A2199. The Rood and Sastry sample was limited at a major-axis diameter of 8″ using a 20-min V exposure. The second sample was limited at a major-axis diameter of 20″ using a 45-min R exposure.

For each individual galaxy a reference line will be defined to pass from the cluster center to the galaxy center. The galaxy major-axis orientation is measured with respect to this line. An angle of 0° indicates that the major axis is parallel to the reference line, and

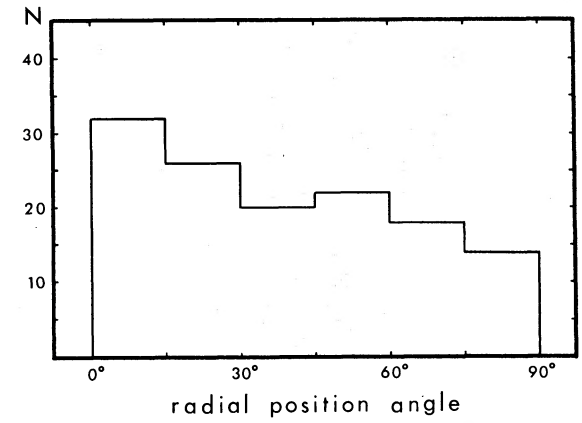

FIG. 4.—Radial position angle distribution for galaxies in the Coma cluster (A1656). Galaxies with major axes pointing toward the cluster core are in the 0° bin, and those with major axes perpendicular to the direction of the cluster core are in the 90° bin.

© American Astronomical Society • Provided by the NASA Astrophysics Data System

1976ApJ...209...22T

hence the galaxy appears to be "pointed" toward the cluster center. An angle of 90° indicates that the major axis is perpendicular to the reference line. For the eight clusters in the present study, only the Coma cluster shows a significant radial alignment trend. The data are plotted in Figure 4. A two-bin χ^2 test can be used to determine the probability that an excess of galaxies will fall in the range 0°–45° and a deficiency in the range 45°–90°. The results are significant at a marginal 10 percent probability level. Note that Coma is the only cluster out of eight which shows this effect. Hawley and Peebles (1975) found the same tendency in their measurements of the Coma cluster, and an earlier report of the same result was made by Gainullina and Roshjakova (1967) for two clusters, Coma (A1656) and Corona Borealis (A2065). Measurements of A2065 have not been confirmed, but it may be significant that both clusters are very rich and apparently symmetrical.

IV. GALAXY ELLIPTICITY DISTRIBUTIONS

Consider first the ellipticity data for each individual cluster sample. Table 3 contains a list of the data, and the normalized ellipticity distributions are plotted in Figure 5. Unfortunately, the number of galaxies per cluster is rather small, so the distributions are poorly defined. It was originally hoped that a comparison between these eight distributions might provide an interesting "homogeneity" test, but the individual samples are just too small to draw meaningful conclusions. Note that the limit on the sample size is intrinsic and not observational. There are simply too few galaxies per cluster larger than $7.5h^{-1}$ kpc to provide a well-defined ellipticity distribution. There are a few conclusions which can be drawn from the data, and these are related to the orientation analysis. Consider what an ellipticity distribution might look like for a system of aligned galaxies. If the aligned system were seen face-on, then the ellipticity distribution should show a strong peak at the low ellipticities. If the aligned system were seen edge-on, then the apparent ellipticity distribution would be identical to the intrinsic one; strong peaks should be seen for disk galaxies at $\epsilon = 6.5$, and the E galaxies should contribute to a flat distribution between $\epsilon = 0$ and $\epsilon \simeq 3.5$.

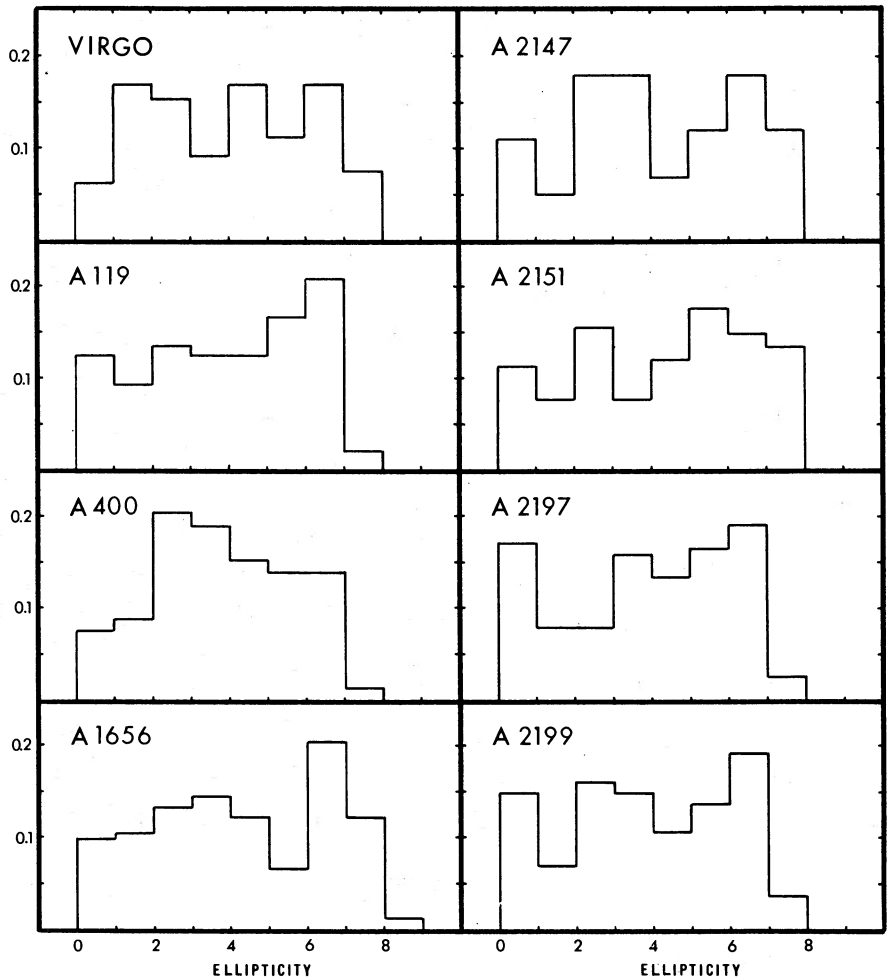

FIG. 5.—Frequency distributions of apparent galaxy ellipticity for the eight clusters studied

© American Astronomical Society • Provided by the NASA Astrophysics Data System

1976ApJ...209...22T

TABLE 3

Ellipticity Distributions for Each Cluster Sample

Number Distributions

Cluster	0	1	2	3	4	5	6	7	8	Total
Virgo	4	11	10	6	11	7	11	5	0	65
A119	12	9	13	12	12	16	20	2	0	96
A400	6	7	16	15	12	11	11	1	0	79
A1656	15	16	20	22	18	10	31	18	2	152
A2147	13	6	21	21	8	14	21	14	0	118
A2151	16	11	22	11	17	25	21	19	0	142
A2197	26	12	12	24	20	25	29	4	0	152
A2199	24	11	26	24	17	22	31	6	0	161

Normalized to $\Sigma = 100$

Cluster	0	1	2	3	4	5	6	7	8	Total
Virgo	6.2	16.9	15.4	9.2	16.9	10.8	16.9	7.7	0	100
A119	12.5	9.4	13.5	12.5	12.5	16.7	20.8	2.1	0	100
A400	7.6	8.9	20.3	19.0	15.2	13.9	13.9	1.3	0	100
A1656	9.9	10.5	13.2	14.5	11.8	6.6	20.4	11.8	1.3	100
A2147	11.0	5.1	17.8	17.8	6.8	11.9	17.8	11.9	0	100
A2151	11.3	7.7	15.5	7.7	12.0	17.6	14.8	13.4	0	100
A2197	17.1	7.9	7.9	15.8	13.2	16.4	19.1	2.6	0	100
A2199	14.9	6.8	16.1	14.9	10.6	13.7	19.3	3.7	0	100

None of the clusters show strong evidence for face-on alignment, although A400 deserves further investigation. Finally, the distribution for A2197 is at least not inconsistent with the approximate edge-on alignment.

To increase the statistical reliability, a composite cluster sample can be formed by combining the data for all clusters into a single sample. Because the ellipticity analysis is critically dependent on the assumption that all galaxies are seen in random orientations, the galaxies in the cluster A2197 will not

TABLE 4

Ellipticity Distribution for Each Morphological Type

Number Distribution

Ellip.	E	E/S0	S0	S0/S	S	S/Irr	Irr	Pec.	Total
0	25	7	29	7	21	0	1	0	90
1	14	7	25	5	17	1	2	0	71
2	18	19	36	12	34	3	4	2	128
3	11	15	33	14	29	4	3	2	111
4	8	6	20	19	32	6	4	0	95
5	1	2	19	28	48	5	2	0	105
6	0	1	24	41	70	6	3	1	146
7	0	0	4	7	49	2	2	1	65
8	0	0	0	0	2	0	0	0	2
Total	77	57	190	133	302	27	21	6	813

Frequency Distribution

Ellip.	E	E/S0	S0	S0/S	S	S/Irr	Irr	Pec.	Total
0	32.5	12.3	15.3	5.3	7.0	0	4.8	0	11.1
1	18.2	12.3	13.2	3.8	5.6	3.7	9.5	0	8.7
2	23.4	33.3	18.9	9.0	11.3	11.1	19.0	33.3	15.7
3	14.3	26.3	17.4	10.5	9.6	14.8	14.3	33.3	13.7
4	10.4	10.5	10.5	14.3	10.6	22.2	19.0	0	11.7
5	1.3	3.5	10.0	21.1	15.9	18.5	9.5	0	12.9
6	0	1.8	12.6	30.8	23.2	22.2	14.3	16.7	18.0
7	0	0	2.1	5.3	16.2	7.4	9.5	16.7	8.0
8	0	0	0	0	0.7	0	0	0	0.2

© American Astronomical Society • Provided by the NASA Astrophysics Data System

1976ApJ...209...22T

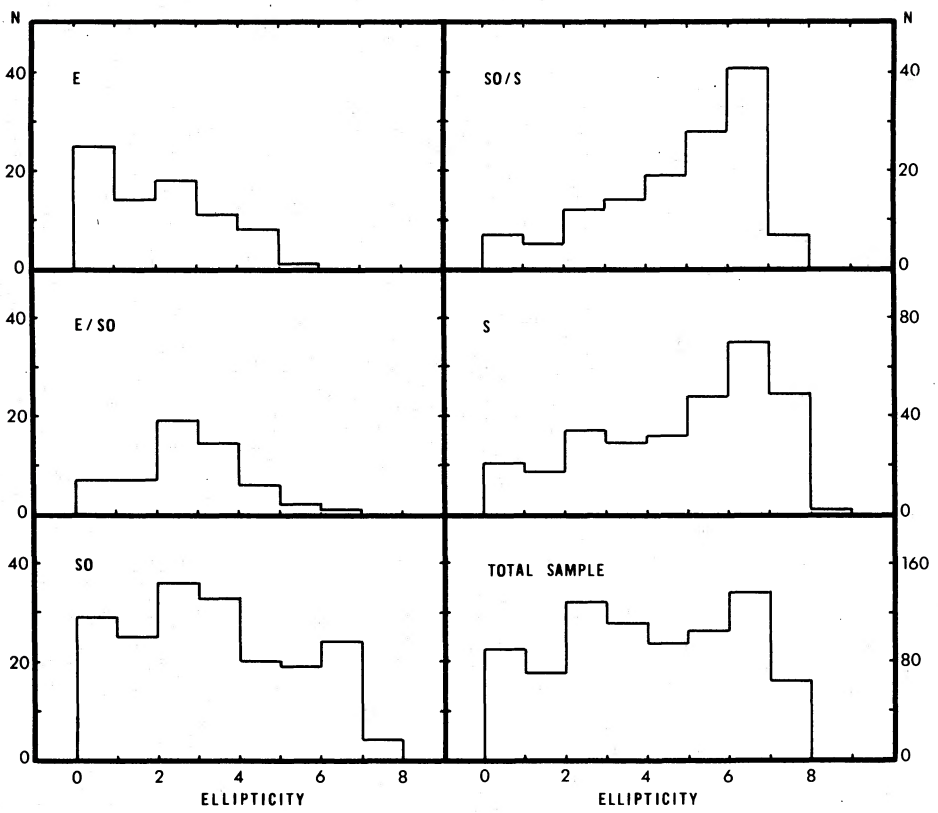

FIG. 6.—Histogram plot showing the number distribution of apparent galaxy ellipticity for the composite sample of galaxies in all clusters except A2197.

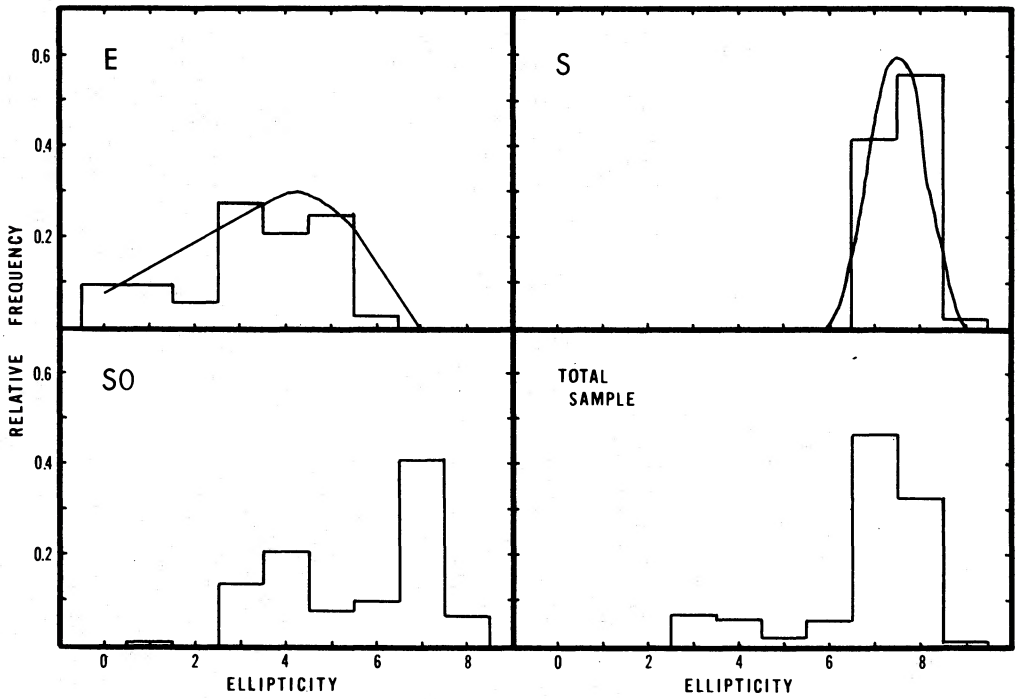

FIG. 7.—Frequency distributions of intrinsic galaxy ellipticity derived from the data shown in Fig. 6

© American Astronomical Society • Provided by the NASA Astrophysics Data System

1976ApJ...209...22T

TABLE 5

Diameter Separation of Galaxy Ellipticity

Number Distributions

Ellip.	Sm.E	Lg.E	Tot.E	Sm.S0	Lg.S0	Tot.S0	Sm.S	Lg.S	Tot.S
0	14	11	25	12	17	29	12	9	21
1	4	10	14	8	17	25	7	10	17
2	9	9	18	14	22	36	16	18	34
3	8	3	11	20	13	33	20	9	29
4	6	-	8	15	5	20	17	15	32
5	1	-	1	13	6	19	26	22	48
6	-	-	-	18	6	24	37	33	70
7	-	-	-	2	2	4	25	24	49
8	-	-	-	-	-	-	1	1	2
Total	42	35	77	102	88	190	161	141	302

Frequency Distributions

Ellip.	Sm.E	Lg.E	Tot.E	Sm.S0	Lg.S0	Tot.S0	Sm.S	Lg.S	Tot.S
0	33.3	31.4	32.5	11.8	19.3	15.3	7.5	6.4	7.0
1	9.5	28.6	18.2	7.8	19.3	13.2	4.3	7.1	5.6
2	21.4	25.7	23.4	13.7	25.0	18.9	9.9	12.8	11.3
3	19.0	8.6	14.3	19.6	14.8	17.4	12.4	6.4	9.6
4	14.3	5.7	10.4	14.7	5.7	10.5	10.6	10.6	10.6
5	2.4	-	1.3	12.7	6.8	10.0	16.1	15.6	15.9
6	-	-	-	17.6	6.8	12.6	23.0	23.4	23.2
7	-	-	-	2.0	2.3	2.1	15.5	17.0	16.2
8	-	-	-	-	-	-	0.6	0.7	0.7

be considered below. In the remaining seven clusters there are 813 galaxies. These will form the basis of the following analysis. The results for this composite cluster sample are given in Table 4 and Figure 6. For the first time the data are seen separated according to morphological type, and a short comment should be made concerning the reliability of the morphological classifications. Although these classifications were made using the KPNO Sky Survey plate copies, three techniques were used to increase the reliability. First, independent classifications were made from good plate material in the centers of the Coma and Hercules (A2151) clusters, and these classifications were used to evaluate what a low-resolution image might show. This technique could be compared with the method of low-resolution spectral classification. Second, the density profile of each galaxy was inspected using the CRT display of a Grant machine. This was very useful in distinguishing between E's and S0's. Third, intermediate classes E/S0 and S/S0 were used as receptacles for galaxies which appeared to be intermediate and therefore defied classification. This makes the three classes, E, S0, and S (spiral), purer and more reliable.

The apparent ellipticity distributions shown in Figure 6 can be used to determine the intrinsic ellipticity distributions for each of the galaxy types (cf. Sandage, Freeman, and Stokes 1970). The results are shown as histograms in Figure 6 for E, S0, and S galaxies plus the total sample. The figure also shows the distributions obtained by Sandage *et al.* (1970) for the de Vaucouleurs' *Reference Catalogue of Bright Galaxies*. This sample could be considered as a "field sample" with a partial contamination from the Virgo cluster. The comparison shows that for E and S galaxies the respective "field" and cluster ellipticity distributions are essentially identical to one another. The Sandage *et al.* study claimed to show that the S0 ellipticity distribution was almost identical to the S distribution. The results shown in Figure 7 indicate a substantial difference, with S0's contributing to two intrinsic ellipticity peaks, one at $\epsilon = 7$ and the other at $\epsilon = 3.5$. While there is a slight possibility that the morphological classifications are producing confusion in the data, a hint of this double peak can be seen in the data used by Sandage *et al.* (compare Fig. 6 of this study with Fig. 1 in Sandage *et al.* 1970), and recent work by de Vaucouleurs (1974) suggests the same conclusion.

The ellipticity data can also be divided according to the galaxies' face-on diameters. Data presented in Table 5 and Figure 8 show a comparison of ellipticity distributions for large and small E, S0, and S galaxies. The large galaxies have $D(O) > 12h^{-1}$ kpc. This diameter limit was chosen in order to make the samples of large and small galaxies approximately equal in size. The two samples of E and S galaxies show nearly identical distributions, but the two S0 samples are quite different. For S0 galaxies, the apparent ellipticity data have been converted to intrinsic ellipticity distributions and the results are given in Figure 9. It appears that the secondary ellipticity peak at $\epsilon \approx 3.5$

© American Astronomical Society • Provided by the NASA Astrophysics Data System

1976ApJ...209...22T

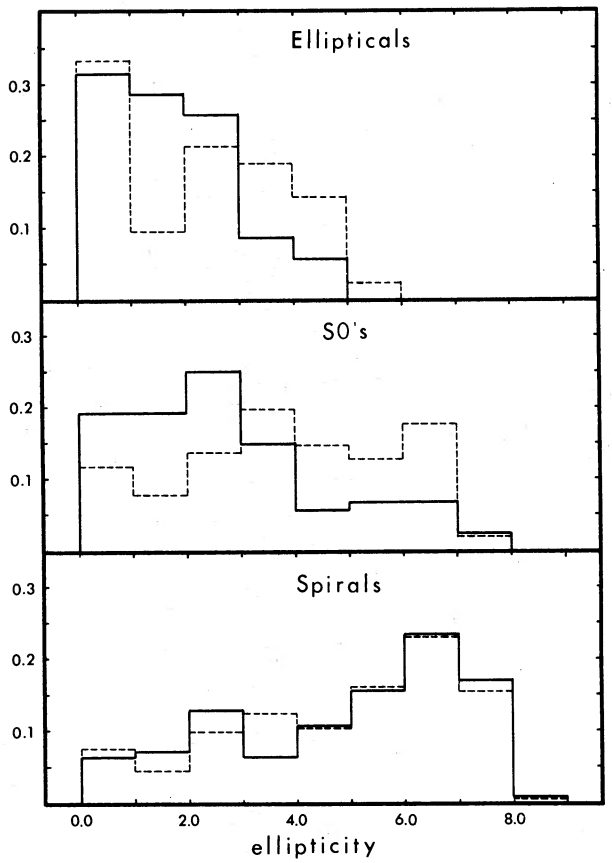

FIG. 8.—Apparent ellipticity distributions for large and small E, S0, and spiral galaxies. The dashed curves show the data for the small galaxies ($D[O] < 12h^{-1}$ kpc), and the solid curve the data for the large galaxies.

may be a characteristic of the larger S0 galaxies, and that the smaller S0's may have an ellipticity distribution more similar to spiral galaxies.

V. DISCUSSION

Before proceeding to an interpretation of the results, it is important to demonstrate that a galaxy's primordial angular momentum vector is nearly identical to the angular momentum vector observed today. The angular momentum of any system can be changed only by applying external torques, and for galaxies this occurs most effectively during violently disruptive collisions. While it is difficult to determine exactly how many close collisions every galaxy has had in its lifetime, statistical arguments can be used to place an upper limit on the average collision frequency. The collision frequency ω depends on the galaxy velocity v, on the collision impact parameter b, and the number density ρ_{CL} of colliding objects (i.e., galaxies). Over the age of the universe t, the total number of collisions per galaxy will be

$$N = \omega t = \frac{3\sqrt{2}}{4} v a^2 \rho_{CL} t \,. \qquad (3)$$

An upper limit to N can be found by evaluating the

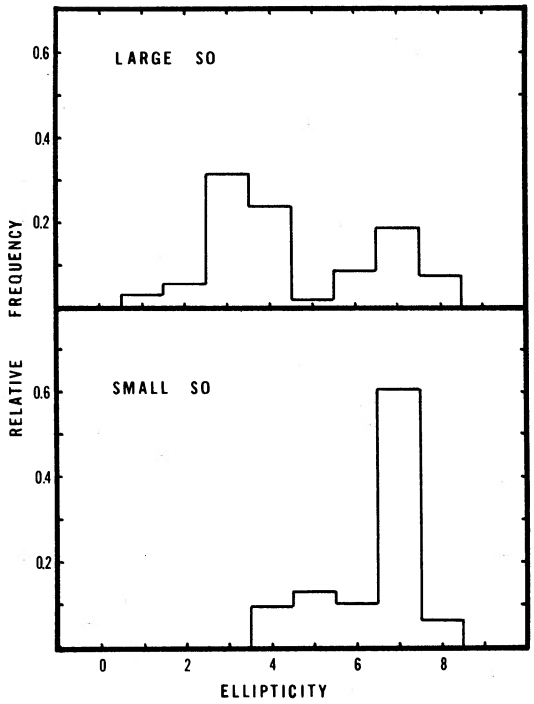

FIG. 9.—Frequency distributions of intrinsic galaxy ellipticity for large and small S0 galaxies. The two samples are separated at a diameter limit $D(O) = 12h^{-1}$ kpc.

expression for parameters characteristic of the Coma cluster. If we take $v \approx 800$ km s^{-1}, $b = 10h^{-1}$ kpc (Alladin, Potdar, and Sastry 1975), $\rho_{CL}(r < 100') = 25h^3$ Mpc^{-3}, and $t = 6.6/h \times 10^9$ yr, then $N = 0.015$. Therefore, only 1.5 percent of all galaxies in Coma should have experienced interpenetrating collisions. Note that the value of ρ_{CL} was chosen to be a mean value over the central portion of the cluster with $r < 100'$ (Abell 1965). The cluster core density is 10 to 20 times larger, so those galaxies which continually pass through the core should experience a substantially larger collision frequency. The slight tendency for radial alignment in Coma might be explained by the disruption of those galaxies which travel on radial orbits through the cluster core. If the disruption causes these galaxies to become extended in their direction of motion, then they should appear to "point" toward the cluster center. Since the collision remnants would be stripped of all gas, they may have a tendency to look like E galaxies as soon as they relax from the initial disruption. It is interesting to see whether the E galaxies in Coma are responsible for the radial alignment effect. Of the 93 S0, S/S0, and S galaxies in Coma, 47 have a radial position angle RPA < 45° and 46 have RPA > 45°. But for the 31 E and E/S0 galaxies, 24 have RPA < 45° and only seven have RPA > 45°. This result is very strong evidence for the disruption of certain Coma cluster galaxies, but recall that none of the other seven clusters show any radial alignment trends. Perhaps only in Coma is the central density sufficiently large or the galaxy orbits sufficiently radial to produce a significant number of disruptive collisions. It is well

© American Astronomical Society • Provided by the NASA Astrophysics Data System

1976ApJ...209...22T

known that the richest and most symmetrical galaxy clusters contain a larger percentage of E galaxies than the average "field" population (cf. Abell 1965). Disruptive collisions may be responsible for producing a certain portion of these elliptical galaxies, and the radial position angle test is a good method of confirming this hypothesis.

A second external torque which acts on cluster galaxies is produced by the tidal influence of the cluster core. If a galaxy were to act as a solid body, this tidal torque would induce a precession of the angular momentum vector. Instead, the stars are free to respond independently and so, rather than reorienting the entire galaxy, the external torque will tend to thicken or destroy any organized stellar disk. To estimate the importance of the external torque, the frequency of precession Ω can be compared with the age of the universe. The precession frequency is

$$\Omega = 2/3 G \rho_{CL} P \sin 2\theta ,$$

where G = gravitational constant, ρ_{CL} = mean cluster density interior to the "precessing" galaxy, P = rotation period of a star in the galaxy, and θ = the angle between the angular momentum vector and the direction to the cluster core. Taking the age of the universe to be $6.6/h \times 10^9$ yr, $P = 2.5 \times 10^8$ yr, $\rho_{CL}(r < 100') = 1.8 \times 10^{-27} h^2$ g cm^{-3} (the dynamic mass density of Coma [Peebles 1971*b*]), and $\theta = \pi/4$, then the number of precession periods over the age of the universe will be

$$N = 0.065h .$$

Note that if N is as large as 0.5, a galaxy's disk will be disrupted. Since the density in the central region of the Coma cluster is 10 to 20 times larger than the value of ρ_{CL} adopted above, this process may be effective in altering the structure of galaxies located near the cores of rich clusters. Tidal precession may be another mechanism which increases the apparent frequency of E galaxies in the richest clusters, and it may be in part responsible for producing the secondary S0 ellipticity peak at $\epsilon = 3.5$.

Since these external torques should have little effect on most cluster galaxies, the alignment trend in A2197 can be interpreted as evidence for a large-scale primordial organization of galaxy angular momentum vectors. But why does this trend show up in only one cluster out of eight? Is there something special about A2197? Looking back at the cluster classifications in Table 1, it appears that A2197 is the only cluster classified L by Rood and Sastry (1972). L means that the brightest galaxies in the cluster are distributed in a *linear* form, and that many of the fainter galaxies are concentrated along the line. This distinction is even more intriguing since the major-axis position angle of the *cluster* is approximately 100°, which is almost identical to the orientation galaxy position angle peak. A second distinctive feature of A2197 is its nearness to A2199. The two clusters have very similar mean redshifts, and they are separated in the sky by only 1°20′.

The relationship between the A2197 cluster orientation and galaxy orientation follows closely the predictions made by cluster collapse models of Sunyaev and Zel'dovich (1972), Doroshkevich (1973*a*, *b*), and Icke (1973). According to these models, the first mass scales to become unstable to Jeans collapse are those associated with galaxy cluster masses. As these masses collapse, galaxy fragmentation occurs whenever the density exceeds a critical value. If the collapse process is symmetrical, then the angular momentum distribution should be isotropic. If the collapse process is asymmetrical and galaxy fragmentation is delayed until the cluster mass collapses into a disk, then galaxy alignment is predicted.

Although the orientation effects in A2197 should not be used as sole support of these models, there is another bit of evidence indicating a similar cluster-galaxy orientation relation. Sastry (1968) found that in five of seven cases cD galaxy position angles were nearly identical to the position angle of the overall cluster in which the cD's were found. The theoretical models of cluster collapse would become even more convincing if just one or two more examples like A2197 could be found. The first clusters that should be searched are those classified L or F (linear or flattened) in the Rood and Sastry system. Although it may be necessary for the cluster to be L or F to show galaxy alignment, this condition may not be entirely sufficient. N-body cluster collapse models by Aarseth (1969) show that even an initially spherical distribution of galaxies can temporarily appear to be linear.

In § IV only brief attention was given to the homogeneity question, i.e., are galaxies of all ellipticities well mixed in space, or are there some regions which contain a larger portion of either flattened or spherical galaxies? The meager conclusions are based on the cluster ellipticity distributions shown in Figure 5, and within the limits of the data it appears that all cluster samples are similar to one another. Having shown in § IV that the intrinsic ellipticity for a galaxy of a particular morphological type is independent of its membership or nonmembership in a cluster, it should be possible to make the homogeneity test using only galaxy morphology data. Two effects are important: (1) How does the relative proportion of disk and non-disk (i.e., elliptical) galaxies change from cluster to cluster? (2) How does the relative proportion change radially within a single cluster? Although these two questions could be answered with fair reliability using the morphology data obtained in the present study, the analysis will be postponed until more detailed galaxy morphology data are available from plates taken with the Mayall 4 m telescope (Gregory and Thompson 1976).

To help determine how galaxies obtained their primordial angular momentum, further work is needed in three areas: (1) galaxy alignment, (2) morphological comparisons among individual cluster samples, and (3) studies of the radial variations of galaxy morphology within single clusters. At the present time, it seems most important to confirm the A2197 alignment effect and then, if possible, find a similar effect in other groups and clusters of galaxies.

© American Astronomical Society • Provided by the NASA Astrophysics Data System

1976ApJ...209...22T

REFERENCES

Aarseth, S. J. 1969, *M.N.R.A.S.*, **144**, 537.
Abell, G. O. 1965, *Ann. Rev. Astr. and Ap.*, **3**, 1.
Alladin, S. M., Potdar, A., and Sastry, K. S. 1975, in *IAU Symposium 69, Dynamics of Stellar Systems*, ed. A. Hayli (Boston: Reidel), p. 167.
Bautz, L. P., and Morgan, W. W. 1970, *Ap. J. (Letters)*, **162**, L149.
Brown, F. G. 1964, *M.N.R.A.S.*, **127**, 517.
———. 1968, *M.N.R.A.S.*, **138**, 527.
Burbidge, G. R., and Burbidge, E. M. 1959, *Ap. J.*, **130**, 629.
de Vaucouleurs, G. 1974, in *IAU Symposium 58, The Formation and Dynamics of Galaxies*, ed. J. R. Shakeshaft (Boston: Reidel), p. 13.
Doroshkevich, A. G. 1973*a*, *Astrofizika*, **6**, 320.
———. 1973*b*, *Soviet Astr.—AJ*, **16**, 986.
Field, G. B. 1965, in *Stars and Stellar Systems*, Vol. **9**, *Galaxies and the Universe*, ed. A. and M. Sandage and J. Kristian (Chicago: University of Chicago Press).
Gainullina, R. Kh., and Roshjakova, T. V. 1967, *Trudy Inst. Ap. Akad. Nauk. Kazaks. S.S.R.*, **5**, 237.
Gregory, S. A., and Thompson, L. A. 1976, in preparation.
Hawley, D. L., and Peebles, P. J. E. 1975, *A.J.*, **80**, 477.
Heidmann, J., Heidmann, N., and de Vaucouleurs, G. 1972, *Mem. R.A.S.*, **75**, 85.
Holmberg, E. 1946, *Medd. Lund Obs.* (II), No. 117.
Hoyle, F. 1949, *Problems of Cosmological Aerodynamics* (International Union of Theoretical and Applied Mechanics and IAU), p. 195.
Icke, V. 1973, *Astr. and Ap.*, **27**, 1.
Jones, B. T. J. 1973, *Ap. J.*, **181**, 269.
Kristian, J. 1967, *Ap. J.*, **147**, 864.
Öpik, E. J. 1968, *Irish A.J.*, **8**, 229.
Ozernoi, L. M., and Chernin, A. D. 1968, *Soviet Astr.—AJ*, **11**, 907.
———. 1969, *Soviet Astr.—AJ*, **12**, 901.
Peebles, P. J. E. 1969, *Ap. J.*, **155**, 393.
———. 1971*a*, *Astr. and Ap.*, **11**, 377.
———. 1971*b*, *Physical Cosmology* (Princeton: New Jersey, Princeton University Press), pp. 67–69.
Rood, H. J., and Baum, W. A. 1967, *A.J.*, **72**, 398.
Rood, H. J., and Sastry, G. N. 1971, *Pub. A.S.P.*, **83**, 313.
———1972, *A.J.*, **77**, 451.
Sandage, A., Freeman, K. C., and Stokes, N. R. 1970, *Ap. J.*, **160**, 831.
Sastry, G. N. 1968, *Pub. A.S.P.*, **80**, 252.
Silk, J., and Lea, S. 1973, *Ap. J.*, **180**, 669.
Sunyaev, R. A., and Zel'dovich, Ya. B. 1972, *Astr. and Ap.*, **20**, 189.
Thompson, L. A. 1974, Ph.D. dissertation, University of Arizona.
von Weizsäcker, C. F. 1951, *Ap. J.*, **114**, 165.

LAIRD A. THOMPSON: Kitt Peak National Observatory, P.O. Box 26732, Tucson, AZ 85726

© American Astronomical Society • Provided by the NASA Astrophysics Data System